Analytical Methods

Accepted Manuscript

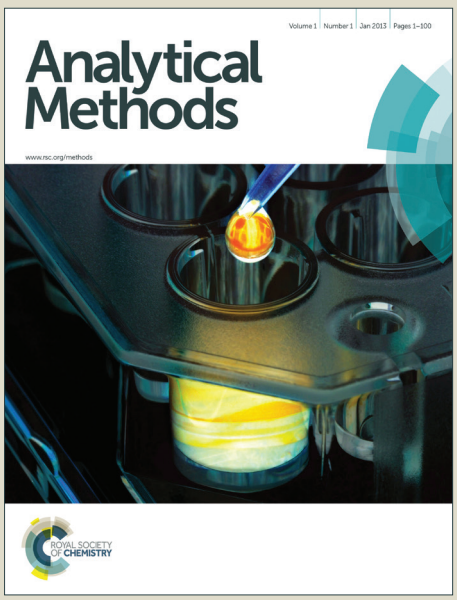

This is an *Accepted Manuscript*, which has been through the Royal Society of Chemistry peer review process and has been accepted for publication.

Accepted Manuscripts are published online shortly after acceptance, before technical editing, formatting and proof reading. Using this free service, authors can make their results available to the community, in citable form, before we publish the edited article. We will replace this *Accepted Manuscript* with the edited and formatted *Advance Article* as soon as it is available.

You can find more information about *Accepted Manuscripts* in the Information for Authors.

ROYAL SOCIETY OF CHEMISTRY

www.rsc.org/methods

Molecularly imprinted surface plasmon resonance (SPR) based sensing of bisphenol A for its selective detection in aqueous systems

Huma Shaikh[a], Gulsu Sener[b], Najma Memon[a], Muhammad Iqbal Bhanger[c], Shafi Muhammad Nizamani[a], Recep Üzek[b], Adil Denizli[b*]

[a] National Center of Excellence in Analytical Chemistry, University of Sindh, Jamshoro 76080, Pakistan.
[b] Department of Chemistry, Biochemistry Division, Hacettepe University, Ankara, Turkey
[c] International Center for Chemical and Biological Sciences. University of Karachi, Karachi -75270, Pakistan.

ABSTRACT

Bisphenol A (BPA) imprinted poly(ethylene glycol dimethacrylate-N-methacryloyl-L-phenyl alanine-vinyl imidazole) [poly(EGDMA-MAPA-VI)] film deposition on SPR sensor with improved efficiency is described in this paper. The molecularly imprinted SPR sensor was characterized by FTIR-ATR, atomic force microscopy and elipsometry. A water-compatible molecularly imprinted film has been developed for rapid, sensitive, and label-free detection of BPA in aqueous solutions prepared in milli Q water, tap water and synthetic wastewater. The real-time response allows detection of BPA with concentrations ranging from 0.08 to 10 μg L^{-1} with LOD and LOQ values of 0.02 and 0.08 μg L^{-1} in milli Q water, 0.06 and 0.2 μg L^{-1} in tap water and 0.08 and 0.3 μg L^{-1} in synthetic wastewater, respectively. A significant increase in sensitivity was therefore expected due to the use of imprinted poly(EGDMA-MAPA-VI) thin film. The method showed good recoveries and precision for the samples spiked with BPA. The results suggest that the imprinted SPR sensing method can be used as a promising alternative for the detection of BPA. The sensor data fitted well with the Langmuir adsorption model. The selectivity studies showed that the imprinted cavities formed in the polymeric nanofilm recognize BPA preferentially rather than 4-nitrophenol, hydroquinone, phenol and 8-hydroxy quinoline with a relative selectivity coefficient of 2.5, 2.6, 2.7 and 2.5, respectively. The prepared BPA imprinted SPR sensor enables high sensitivity, label-free detection, real-time monitoring, low volume sample consumption, quantitative evaluation, and determination of kinetic rate constants very well. In addition, SPR based BPA sensor is easy to perform and can

be a cost effective solution due to the reusability of the prepared sensor. Furthermore, storage stability will be longer than antibody-based detection methods.

Keywords: Bisphenol A; Molecular imprinting; Surface plasmon resonance sensor; Label-free detection.

Corresponding Author: Prof. Adil Denizli, email: denizli@hacettepe.edu.tr

Co-corresponding Author: Dr. Najma Memon, email: najmamemon@gmail.com

Author: Huma Shaikh, email: huma.hashu@gmail.com

Co-authors: Prof. Muhammad Iqbal Bhanger, email: dbhanger2000@gmail.com

Prof. Shafi Muhammad Nizamani, email: drshafi.nizamani@gmail.com

1. Introduction

Endocrine disruptors lead to adverse health effects in humans and wildlife because of their ability to cause changes in endocrine function. Due to its estrogenic properties BPA (2,2-bis(4-hydroxyphenyl) propane) is among the chemicals recognized as a potential endocrine disruptor. Animals based laboratory studies have focused on revealing the estrogenic activity and adverse effects of BPA [1]. Epigenetic effects of BPA have also been confirmed [2,3]. The increased risks of cardiovascular diseases, liver-enzyme abnormalities and diabetes mellitus are suspected even at low dose of BPA [4].

Studies revealed that BPA is released from polycarbonates flasks, food cans [5], dental sealants [6] and hemodialyzers [7,8]. Murakami *et al.,* [9] reported that the patients going through the dialysis are at potential health risk due to elution of BPA from polycarbonate plastics and epoxy resins used in hemodialysis systems.

BPA is one of the chemicals produced in maximum volume world wide [10]. It is predicted that global demand for BPA has grown from 3.9 million tons in 2006 to approximately 5 million tons in 2010. Germany, the Netherlands, the USA, Japan and many other countries have large capacities for the production of BPA [11]. It is also used for the production of unsaturated polyester resins and polyacrylate, polyetherimide and polysulphone resins and flame retardants [12]. The extensive use of BPA-based polymers, with ester bonds subject to hydrolysis and non-polymerized monomer residues, has led to widespread environmental contamination. BPA concentrations in the ranges 5–320 ng L^{-1} in river waters [13], 20–700 ng L^{-1} in sewage effluents [14], 2–208 ng m^{-3} in air, 0.2–199 ng g^{-1} in dust [15] and 0.1–384 ng g^{-1} in foodstuffs [16] have been reported.

A range of methods and technologies have been developed to determine BPA recently. These methods mainly include fluorescence spectrometry [17], gas chromatography–mass spectrophotometry [18], gas chromatography [19], high-pressure liquid chromatography [20], liquid-chromatography mass spectrophotometry [21], enzyme linked immunosorbent assay [22], and capillary electrophoresis [23]. Though, these detection methods are usually time consuming and difficult, often involving the assistance of specialized technicians and the employment of costly testing equipment. Also, the complexed labeling procedure may also disrupt the function of biological molecules. Furthermore, these methods do not offer real time analysis of BPA which

is the utmost requirement due to its high dissemination in the environment. Consequently, the development of a label-free, simple, fast, real time and low-cost detection method is essential.

Thus, the area of sensors for the detection of BPA has been widely explored and several types of chemical and biosensors have been developed. Researchers are still working hard to develop the most relaiable and feasible sensors for BPA. The phenolic groups in BPA molecule make it active electrochemically but its direct determination is complicated due to weak response of BPA in conventional electrochemical sensors. Numerous electrochemical sensor fabricated with advanced materials have been developed to increase the surface area of electrode to enhance oxidation signals [24,25]. Optical sensors are known for their simplicity, low cost, efficiency, and accuracy. However the use of surface plasmon resonance (SPR) immunosensors are very common for detection of trace level of BPA [26,27] but these sensors are not proved to be cost effective and robust. In general, SPR does not show the same degree of high sensitivity toward detection of small molecules such as BPA [28], as it does for macromolecules such as proteins and DNA. Molecular imprinting technique is playing a better role in producing sensitive SPR sensors [29,30]. The imprinted SPR sensor selective for BPA was reported by Taguchi *et al.,* [31] recently. The gold NPs were used to enhance the response of sensor. Thus there is a need to develop highly sensitive, robust and simple SPR sensor for the detection of BPA.

In order to accomplish the above mentioned goals we focused on producing a highly selective, simple and real time detection method based on SPR sensor for BPA. We made an effort to produce an effective and straightforward combination of molecular imprinting and SPR sensor technique. Thus the BPA imprinted poly(EGDMA-MAPA-VI) nanofilm was deposited on SPR chip to carry a real time detection of BPA in aqueous systems of diverse origin. The kinetic and isotherm parameters of BPA imprinted SPR sensor were calculated by applying Association kinetics analysis, Scatchard, Langmuir, Freundlich and Langmuir-Freundlich isotherms. The molecularly imprinted poly(EGDMA-MAPA-VI) nanofilm was characterized by FTIR-ATR, AFM and ellipsometery in terms of structural properties, surface morphology and thickness. Further, the analytical performances of BPA imprinted SPR sensor were evaluated with respect to sensitivity, linearity and selectivity, etc. It was observed that the molecularly imprinted poly(EGDMA-MAPA-VI) nanofilm based SPR chip could specifically recognize and detect

BPA to lower limits of detection. Furthermore, it was rugged and robust with reasonable reusability and precision.

2. Experimental

2.2. Chemicals and reagents

All solvents/reagents used for the synthesis and preparation of solutions were of analytical grade. Sulphuric acid (H_2SO_4, 99.9%), sodium hydroxide (NaOH, 98%) and hydrogenperoxide (H_2O_2), were purchased from Merck, Germany. Ethyl acetate, ether, cyclohexane and ethanol were purchased from Fisher Scientific, UK. BPA, 4-nitrophenol, hydroquinone, phenol, 8-hydroxy quinoline, L-phenylalanine, sodium nitrite ($NaNO_2$), potassium carbonate (K_2CO_3), ethylene glycol dimethacrylate (EGDMA), allyl mercaptane (CH_2CHCH_2SH), 1-vinyl imidazole (VI), 2,2´-azobis(2-methylpropionitrile) (AIBN, 98%), trimethylchlorosilane and methacryloyl chloride were obtained from Sigma-Aldrich, Finland. The deionized water purified by a Millipore Milli-Q Plus water purification system (Elga model classic UVF, UK) was used to prepare aqueous solutions.

2.3. Surface characterization of SPR sensor

Thermo Fisher Scientific, Nicolet iS10, Waltham, MA, USA (spectral range from 4000 to 400 cm^{-1}) FTIR-ATR spectrophotometer was used to record FTIR-ATR spectra. Atomic force microscope Nanomagnetics Veeco 5A was used for surface characterization. Estimation of thickness of polymeric nanofilm on SPR sensor was carried out through Accurion EP3 Imaging Ellipsometer, Lastek (photonics technology solutions), Australia.

2.4. Apparatus

Surface plasmon resonance system SPRi-Lab GenOptics, Orsay, France was used to carry out all the studies of SPR sensors. Gold-coated (thickness 50 nm) SPR chips (25 mm×12.5 mm) provided by GenoOptics were coated with nanofilms.

2.5. Synthesis of N-methacryloyl-L-phenylalanine (MAPA) monomer

N-methacryloyl-L-phenylalanine (MAPA) was synthesized by following the elsewhere reported method [32]. Precisely, the mixture of L-phenylalanine (5.0 g) and $NaNO_2$ (0.2 g) was prepared by

dissolving them in 30 mL of K_2CO_3 aqueous solution (5%, w/v). The mixture was maintained at 0 °C followed by gradual addition of methacryloyl chloride (4.0 mL) under gentle nitrogen stream. The reaction was continued for 2 h with constant magnetic stirring. Finally, the pH of reaction solution was maintained at 7.0 at the completion of reaction. The product was extracted using ethyl acetate and aqueous phase was removed using rotary evaporator. To crystallize the residue (MAPA) ether-cyclohexane mixture was utilized.

2.6. Preparation of BPA imprinted surface plasmon resonance (SPR) sensor

2.6.1. Surface modification of the SPR chips

2.6.1.1. Allyl mercaptane modification

The acidic piranha solution (3:1 H_2SO_4: H_2O_2, v/v) was used to clean SPR chip thoroughly. The cleaning of chip was carried out by immersing it in pirhana solution of 20 mL for 30 sec and in pure ethyl alcohol, respectively. Finally it was dried in vacuum oven (200 mmHg, 40°C) for 3 h. In order to introduce the vinyl groups, the surface modification of SPR chip was carried using allyl mercaptane (CH_2CHCH_2SH). Briefly, the 3.0 M solution of allyl mercaptane was prepared in an ethanol/water mixture (4:1, v/v) and SPR chip was dipped into it for 12 h. At the completion of surface modification the chip was rinsed with ethanol thoroughly and dried in vacuum (200 mmHg, 40°C) under nitrogen stream.

2.6.1.2. Polymer preparation on SPR chip surface

To prepare BPA imprinted polymeric nanofilm on allyl mercaptane modified SPR chip surface, MAPA and VI were used as functional monomers. The polymer solution was prepared as follows: BPA (0.005 g) and MAPA ($1.5x10^{-4}$ g) were dissolved in 50 µL of ethanol followed by the addition of 25 µL of VI. 1 mg of AIBN was dissolved in 125 µL of ethanol and 80 µL of EGDMA was added into the mixture. Finally the monomer solutions were mixed and stock solution was purged with nitrogen to remove dissolved oxygen. The gold surface of SPR chip was kept on the glass lamella surface coated with trimethylchlorosilane and containing stock monomer solution of 2.5 µL. Polymerization was carried under UV light at ambient temperature (100 W, 365 nm) for 30 min. The glass lamella was detached from the surface of chip after completion of polymerization. Polymer coated SPR chip was first washed with 0.2 mM NaOH, rinsed with D.I water and then dried in vacuum oven.

2.6.2. Kinetic studies with SPR chip

The interactions between BPA-imprinted poly(EGDMA-MAPA-VI) nanofilm and BPA molecules were investigated. Milli Q water, tap water samples and synthetic wastewater samples were spiked with different concentrations of BPA and applied to SPR system. BPA-imprinted poly(EGDMA-MAPA-VI) SPR chip was used for kinetic analysis. The summary of experimental process is as follows; the washing of SPR chip was first done with 0.2 mM NaOH solution (10 mL, 1 mL min^{-1} flow rate) and then with deionized water (50 mL, 1 mL min^{-1} flow rate), respectively. The surface plasmon curves were obtained and the resonance angle was calculated while water was circulating. Finally, the mirror system was established at the obtained resonance angle and kinetic studies were further carried at this value of angle to obtain surface plasmon resonance curves. Plasmon curves were attained via SPRview software. The plasmon curves values were examined by SPR1001 software and plotted as the angle of incident light versus percent diffraction amount. For kinetic analysis studies the SPRview software was utilized as kinetic monitoring program. To obtain stable base line water circulation was carried for 5 more minutes and finally the BPA sample was introduced to SPR system (10 mL and 1 mL min^{-1} flow rate). The resonance frequency experienced reflectivity (%) changes as soon as BPA solution reached SPR chip. The resonance frequency reached platue value in approximately 15 min. 0.2 mM NaOH solution was applied to carry desorption of BPA from SPR chip (10 mL and 1 mL min^{-1} flow rate) and finally washing was done using deionized water (50 mL and 1 mL min^{-1} flow rate). Adsorption-desorption-washing steps were repeated for each analysis. The kinetic data was analyzed using SPR1001 software. The kinetic studies were performed to obtain linear range of SPR chip for the determination of BPA in milli Q water, tap water and synthetic wastewater. The kinetic studies were also performed to compare the efficiency of different SPR chips and results are given by presenting RSD values.

3. Results and discussion

3.1. Preparation of BPA imprinted SPR sensor

Figure 1 shows the schematic representation of imprinting of BPA in poly(EGDMA-MAPA-VI) nanofilm on allyl mercaptane modified SPR chip. The allyl mercaptane modification was used as tool to implant imprinted nanofilm on SPR chip surface tightly. The mixed monomer system

comprised of MAPA and VI was expected to produce sensitive and effectively imprinted nanofilm. The results based on kinetic study of SPR reveal that nanofilm is very sensitive and selective. Moreover, the preparation method of BPA imprinted SPR sensor was very simple and quick. The monomers mixture along with BPA was prepared and BPA imprinted polymeric nanofilm was made under UV light (Figure 2). Previously reported BPA sensors were biosensors [33]. However, SPR sensors based on molecular imprinting do not require expensive antibodies. Moreover, they are more robust in wide range of pH and in samples of diverse nature. The shelf life of poly(EGDMA-MAPA-VI) nanofilm based SPR sensor was found good. There was a need to introduce simple and robust method for the preparation of BPA imprinted SPR sensor, thus we focused on the selection of appropriate functional monomers because effective imprinting can overcome the problem of sensitivity of sensor and enhances the selectivity. Mixed monomer system was used to interact with BPA, MAPA and VI produced very sensitive sensor, highly selective for BPA. Furthermore, the synthesis method of imprinted nanofilm was reproducible and lead to the successful production of number of SPR chips with same properties

3.2. Characterisation

3.2.1. FTIR-ATR spectra

FTIR-ATR spectroscopy was used to confirm polymerization process. The specific bands of the polymeric structure were determined as carbonyl band from amide that can be seen in the region of 1700 cm^{-1}. However it has been shifted from 1721 cm^{-1} in NIP to 1719 cm^{-1} in BPA imprinted nanofilm (MIP), also its intensity is decreased in MIP that shows interaction of carbonyl group of MAPA with BPA in MIP. The –NH stretching band at 3301 cm^{-1} and –CH stretching bands of methyl group at 2938 cm^{-1} and in the region of 2870 cm^{-1} (Figure 3) further confirm the presence of MAPA in polymer. The band in the region of 1650 cm^{-1} and 1500 cm^{-1} are characteristic bands of vinyl imidazole due to N-C=N stretching and C=N stretching, respectively. These bands confirm the presence of vinyl imidazole in polymeric nanofilm. The –CH bending vibrations due to methylene group and C-O stretching vibrations between carbon and hydroxyl group in the region of 1448 cm^{-1} and 1050 cm^{-1}, respectively further confirm the presence of MAPA in polymer. There is a prominent band at around 945 cm^{-1} due to –CH bending vibrations of alkene group from VI.

3.2.2. AFM Studies

The non-contact mode AFM was applied to study the surfaces of unmodified, allyl mercaptane modified and BPA-imprinted thin nanofilm modified SPR chips. AFM images of non-modified, allyl mercaptane modified and BPA imprinted poly(EGDMA-MAPA-VI) thin nanofilm modified SPR chips are given in Figure 4. The 3D-images show that, surface depth value of non-modified SPR chip surface (Figure 4a) was increased from 6.15 nm to 22.82 nm after allyl mercaptane modification (Figure 4b). These results propose that the surface modification with allyl mercaptane was accomplished homogeneously. After the polymerization process, surface depth increased to 68.14 nm (Figure 4c). These results confirm that the roughness of surface was enhanced and polymerization could be accomplished on the surface of SPR chip.

3.2.3. Ellipsometery measurements

In order to estimate exact thickness of polymeric nanofilm SPR chips were further characterized through ellipsometery measurements. All thickness measurements were performed at a wavelength of 658 nm with an angle of incidence of 60°. Measurements were carried out as triplicate at 6 different points of SPR sensor surface, and the results were reported as mean value of the measurements with standard deviations. The thickness of non-modified SPR chip was 11.4 nm, where as its value increased to 92 nm after formation of MIP nanofilm on SPR sensor. Root mean square roughness (RMS) values of the gold surface were also determined. RMS roughness value of the non-modified gold SPR chip, cleaned with acidic piranha solution was determined as 0.8 nm. After the formation of MIP nanofilm, this value increased to 33 nm. These results revealed that the formation of polymeric nanofilm was successfully achieved on the surface of SPR chip. Figure 5 shows the results obtained from ellipsometery measurement.

3.3. Kinetic studies with SPR chip

BPA imprinted SPR chip was used for real time monitoring of the interactions between the molecular imprinted nanofilm and BPA, from aqueous solutions. The SPR chip was interacted with aqueous solutions of BPA in different concentration ranges of 0.01–1000 μg L^{-1}. Figure 6 shows that the change in reflectivity with respect to change in concentration of BPA is linear till 10 μg L^{-1} and SPR chip gains saturation at this concentration. Hence, it does not show further change in reflectivity at higher concentrations. As seen in Figure 7, all steps including equilibration–adsorption–desorption–regeneration were almost completed in 60 min. However,

the sensor reached the plateau value in 15 min which is due to the brilliant affinity of sensor towards BPA. Increase in concentration caused also increase in sensor response. In this study, the change in reflectivity increased from 0.1 to 8.12 for BPA-imprinted SPR chip and from 0.15 to 3.2 for non-imprinted SPR chip.

The BPA imprinted nanofilm has high affinity and ability to recognize BPA as compared to non-imprinted nanofilm (Figure 6). The linearity of the sensor response in the studied concentration range was checked in milli Q water, tap water and synthetic wastewater. It can be seen in Figure 8 that the sample matrix did not affect the sensitivity of BPA-imprinted sensor very much. Not only good linear regression constants were obtained in all samples but also good detection limits i.e. 0.02, 0.06 and 0.08 μg L^{-1} were obtained for milli Q water, tap water and synthetic wastewater. Moreover, satisfactory quantification limits were attained for all types of aqueous samples and sample matrix did not affect the sensitivity of assay. The inter- and intraday precissions were also calculated for three different concentrations such as 0.2, 2 and 10 μg L^{-1} of BPA. The results reveal acceptable RSD values which further indicate that the devised imprinted SPR sensor is robust, reliable and rugged. The percent recovery of the assay was also monitored in lake water spiked with selected concentrations of BPA. The percent recovery of 98.7, 100.6 and 102.7 were obtained for lake water spiked with 0.2, 2 and 10 μg L^{-1} of BPA, respectively. (Table 1). These results show that the BPA imprinted nanofilm based SPR sensor is rugged and reliable. The precission of 6 different SPR chips was also estimated for selected concentrations of BPA. The obtained RSD values were 2.45 %, 2.15 % and 1.14% for 0.2, 2 and 10 μg L^{-1}, respectively. The reasonable RSD values obtained from using different SPR chips indicate that the preparation method of BPA imprinted nanofilm is consistent and robust.

3.4. Analysis of kinetic data

3.4.1. Equilibrium analysis

If the total amount of binding site $[B]_o$ is expressed in terms of the maximum analyte binding capacity of the surface, i.e., the total amount of BPA imprinted binding site on the chip surface, all concentration terms can then be expressed as SPR response signal R, eliminating the need to convert from mass to molar concentration. Under pseudo first order conditions where the free

analyte concentration is held constant in the flow cell, the binding can be described by following equation;

$$\frac{d\Delta R}{dt} = k_a C(\Delta R_{\max} - \Delta R) - k_d \Delta R \quad (1)$$

where dΔR/dt is the rate of change of the SPR response signal, ΔR and $\Delta R_{\max}$ are the measured and maximum response signal measured with binding, C is the injected concentration of the analyte (μg L^{-1}), k_a is the association rate constant (μg^{-1}s^{-1}) and k_d is the dissociation rate (s^{-1}). The binding constant, i.e., association constant K_A, may be calculated as $K_A = k_a/k_d$ (μg L^{-1}). At equilibrium, dΔR/dt=0 and the equation can be rewritten:

$$\frac{\Delta R_{eq}}{C} = K_A \Delta R_{\max} - K_A \Delta R_{eq} \quad (2)$$

Therefore, the steady state association constant K_A can be obtained from a plot of $\Delta R_{eq}/C$ versus R_{eq} and the dissociation constant K_D can be calculated as $1/K_A$.

Eq. (1) may be rearranged to give:

$$\frac{d\Delta R}{dt} = k_a C \Delta R_{\max} - (k_a C + k_d)\Delta R \quad (3)$$

Thus a plot of dΔR/dt against ΔR will theoretically be a straight line with slope $-(k_a C + k_d)$ for interaction-controlled kinetics [34]. Table 2 shows that the obtained value of k_a (0.18 μg L^{-1} s^{-1}) is higher than the value of k_d (0.016 s^{-1}). These results propose that the poly(EGDMA-MAPA-VI) based nanofilm has good affinity for BPA and is capable to bind BPA tightly.

3.4.2. Equilibrium isotherm models

To describe the interaction model between BPA imprinted poly(EGDMA-MAPA-VI) SPR sensor and BPA molecules, four different equilibrium isotherm models were examined to equilibrium data: Scatchard, Langmuir, Freundlich, and Langmuir–Freundlich (LF):

Scatchard $$\frac{\Delta R_{ex}}{[A]} = K_A(\Delta R_{\max} - \Delta R_{eq}) \quad (4)$$

Langmuir $$\Delta R = \{\Delta R_{\max}[A]/K_D + [A]\} \quad (5)$$

Freundlich $$\Delta R = \Delta R_{\max}[A]^{1/n} \quad (6)$$

Langmuir-Freundlich $$\Delta R = \left\{\Delta R_{\max}[A]^{1/n}/K_D + [A]^{1/n}\right\} \quad (7)$$

The equilibrium dissociation constant (K_D) and Freundlich heterogeneity index ($1/n$) are additional parametes. The MIP binding isotherms are commonly fit to the homogeneous binding site Langmuir model [35]. Yet, recent studies propose that MIPs have heterogeneous binding sites [36]. The Freundlich model is one of the heterogeneous models that fit MIP adsorption isotherm data brilliantly at low concentration regions [37], but is unable to reveal saturation performances of MIPs. However, the Langmuir–Freundlich (LF) model provides not only heterogeneity information but is also capable of modeling adsorption behavior over the entire range of concentration from unsaturation to saturation. To prevent the necessity of conversion of mass-concentration parameter, some parameters, Qmax to $\Delta R_{\max}$, Q to ΔR etc., were changed when curves were drawn. Scatchard, Langmuir, Freundlich and Langmuir–Freundlich models were employed to experimental data. The linear fit with the Langmuir equation was comparably the best, which means that the binding of BPA molecules onto imprinted poly(EGDMA-MAPA-VI) SPR sensor is monolayer, although Scatchard curve shows some surface heterogeneity. Similar results were reported by others [35,36]. Surface heterogeneity shown by Scatchard curve is may be because the imprinted poly(EGDMA-MAPA-VI) SPR sensor surface has different binding sites which have different binding affinity to BPA molecules. Then, the monolayer binding of BPA molecules was occurred and the binding process was well-fitted to Langmuir equation. To show multilayer binding of analyte molecules Freundlich model is employed. Linear regression coefficients of Langmuir and Langmuir–Freundlich, isotherms were higher than Freundlich isotherm. The results of Scatchard plot also showed that BPA-imprinted SPR sensor has two types of binding sites i.e. high affinity and low affinity binding sites. The calculated parameters for all models were given in Table 2. The best fitted model to explain the interaction between BPA-imprinted SPR sensor and BPA molecules was Langmuir isotherm (R^2 = 0.9999). The ΔRmax value, calculated by using Langmuir model, was very close to the experimental one (ΔR=8.12).

3.5. Selectivity of BPA imprinted poly(EGDMA-MAPA-VI) SPR sensor.

Selectivity is not only an advantage of MIP, but also a characteristic of any sensor. Therefore, evaluating the selectivity of the MIP nanofilm-coated sensor is highly important. BPA and four structurally related compounds were tested to evaluate the selectivity of the MIP nanofilm. The structures of the five compounds are shown in Figure 9. 4-nitrophenol, hydroquinone, phenol and 8-hydroxy quinoline have structures similar to BPA. The results of the selectivity of the imprinted sensor are shown in Figure 10. For the MIP-coated SPR sensor chip, the responses of the compounds other than BPA were significantly lower. Also the comparison of response of MIP-coated sensor chip to the response of NIP-coated sensor chip shows that MIP has more capacity for BPA. This may be due to the fact that MIP-coated sensor chip has some preferential binding of BPA as compared to the NIP. However, the NIP nanofilm, without the specific recognition sites, resulted in complete nonspecific absorption. Moreover, the responses of the MIP nanofilm to 4-nitrophenol, hydroquinone, phenol and 8-hydroxy quinoline are similar to that of the NIP nanofilm. This similarity can be explained by considering that the MIPs also contain limited number of non-specific binding sites. Thus the binding of 4-nitrophenol, hydroquinone, phenol and 8-hydroxy quinoline onto MIP and NIP SPR sensors is nonspecific.

In SPR sensor applications, the concentration and mass parameters are modified because there is no significant difference between the initial and final concentration of analyte solutions. In addition, the mass of the polymer is not accurately determined and the relationship between ΔR and concentration is linear [38]. Therefore, the selectivity coefficient k is described by the following equation.

$$k = \Delta R_{template} / \Delta R_{competitor} \qquad (8)$$

The equation for relative selectivity coefficient, k′ can be written:

$$k' = k_{MIP} / k_{NIP} \qquad (9)$$

The selectivity coefficients of BPA imprinted SPR chip were calculated and are summarized in Table 3. As summarized in Table 3, the BPA imprinted SPR chip specifically recognizes the

BPA molecules. The selectivity coefficients of the imprinted SPR chip for BPA are 2.5, 2.6, 2.7 and 2.5 according to 4-nitrophenol, hydroquinone, phenol and 8-hydroxy quinoline, respectively.

3.6. Reproducibility of BPA imprinted poly(EGDMA-MAPA-VI) SPR sensor

MIPs have the advantages of robustness and physical and chemical stability. Therefore, the MIP nanofilms also reveal same stability under the diverse physical and chemical conditions. According to the results shown in Figure 11, the SPR angle shifts decreased slightly after 6 cycles, which may be caused by incomplete removal of BPA. The results show that the MIP SPR sensor has good reproducibility.

4. Conclusion

In this work, we have demonstrated a sensitive SPR sensing protocol based on molecular imprinting technique for the detection of BPA. The poly(EGDMA-MAPA-VI) based thin nanofilm highly selective for BPA was prepared on SPR sensor via radical polymerization under UV light. The obtained imprinted MIP sensor reveals the brilliant sensing of BPA which is highly sensitive to minor changes in concentration. In addition, the fast association/dissociation kinetics for template recognition can be observed due to excellent affinity of polymeric nanofilm towards BPA. Therefore, sensitive and selective detection of BPA was achieved by employing the MIP nanofilm as both an amplifier to increase the SPR signal and a special recognition element to improve the selectivity due to its imprinting effect. The wide response range, excellent sensitivity and selectivity, and high stability of the MIP based SPR sensor makes it an attractive recognition tool for detection of BPA.

Acknowledgement:

Authors are grateful to TUBITAK (The scientific and technological research council of Turkey) for providing finanacial support to accomplish this research work.

References

1. Y. B. Wetherill, B. T. Akingbemi, J. Kanno, J. A. McLachlan, A. Nadal, C. Sonnenschein, C. S. Watson, R. T. Zoeller and S. M. Belcher, *Reprod. Toxicol.*, 2007, 24, 178-198.
2. J. A. Dodge, A. L. Glasebrook, D. E. Magee, D.L. Phillips, M. Sato, L. L. Short and H. U. Bryant, *J. Steroid Biochem. Mol.*, 1996, 59, 155-161.
3. G. S. Prins, W. Y. Tang, J. Belmonte and S. M. Ho, *Basic Clin. Pharmacol. Toxicol.*, 2008, 102, 134-138.
4. I. A. Lang, t. S. Galloway, A. Scarlett, W. E. Henley, M. Depledge, R. B. Wallace and D. Melzer, *J. Am. Med. Assoc.*, 2008, 300, 1303-1310.
5. J. A. Brotons, M. F. Olea-Serrano, M. Villalobos, V. Pedraza and N. Olea, *Environ. Health Perspect.*, 1995, 103, 608-612.
6. N. Olea, R. Pulgar, P. Perez, F. Olea-Serrano, A. Rivas, A. Novillo-Fertrell, V. Pedraza, A. M. Soto and C. Sonnenschein, *Environ. Health Perspect*., 1996, 104, 298-305.
7. Y. Haishima, Y. Hayashi, T. Yagami and A. Nakamura, *J. Biomed. Mater Res*., 2001, 58, 209-215.
8. H. Yamasaki, Y. Nagake and H. Makino, *Nephron*, 2001, 88, 376-378.
9. K. Murakami, A. Ohashi, H. Hori, M. Hibiya, Y. Shoji and M. Kunisaki, *Blood Purif*., 2007, 25, 290-294.
10. C. A. Staples, K. Woodburn, N. Caspers, T. Hall and G. M. Klecka, *Hum. Ecol. Risk Asses.*, 2002, 8, 1083-1105.
11. G. Lyons, 2000, Bisphenol, A Known Endocrine Disruptor. Surrey, WWF-UK.
12. O. C. Dermer, 1999, Encyclopedia of Chemical Processing and Design. J. McKelta, J., Weismantel, G.E. New York, Marcel Dekker: 406.
13. A. Ballesteros-Gómez, F. J. Ruiz, S. Rubio and D. Pérez-Bendito, *Anal. Chim. Acta*., 2007, 603, 51-59.
14. D. W. Kolpin, E. T. Furlong, M. T. Meyer, E. M. Thurman, S. D. Zaugg, L. B. Barber and H. T. Buxton, *Environ. Sci. Technol.*, 2002, 36, 1202-1211.
15. N. K. Wilson, J. C. Chuang, M. K. Morgan, R. A. Lordo and L. S. Sheldon, *Environ. Res.*, 2007, 103, 9-20.
16. A. Goodson, W. Summerfield and I. Cooper, *Food Addit. Contam*., 2002, 19, 796-802.
17. J. Fan, H. Q. Guo, G. G. Liu and P. A. Peng, *Anal. Chim. Acta*., 2009, 35, 1096-1107.
18. B. M. Thomson and P. R. Grounds, *Food Addit. Contam. Part A*, 2005, 22, 65-72.
19. C. Chang, C. Chou and M. Lee, *Anal. Chim. Acta*., 2005, 539, 41-47.
20. L. Patrolecco, S. Capri, S. De Angelis, S. Polesello and S. Valsecchi, *J. Chromatogr. A*, 2004, 1022, 1-7.
21. S. N. Pedersen and C. Lindholst, *J. Chromatogr. A*, 1999, 864, 17-24.
22. Y. Feng, B. Ning, P. Su, H. Y. Wang, C. H. Wang, F. S. Chen and Z. X. Gao, *Talanta*, 2009, 80, 803-808.
23. H. Gallart-Ayala, O. Nunez, E. Moyano and M. T. Galceran, M.T, *Electrophoresis*, 2010, 31, 1550-1557.
24. J. Huang, X. Zhang, S. Liu, Q. Lin, X. He, X. Xing, W. Lian, *J. Appl. Electrochem.,* 2011, 4, 1323–1328.
25. D.C. Apodaca, R.B. Pernites, R. Ponnapati, F.R. Del Mundo, R.C. Advincula, *Macromolecules*, 2011, 44, 6669–6682.

26. K. Hegnerová, M. Piliarik, M. Šteinbachová, Z. Flegelová, H. Černohorská and J. Homola, *Anal. Bioanal. Chem*., 2010, 398, 1963-1966.
27. N. A. Bakar, M. M. Salleh, A. A. Umar and M. Yahaya, *Key Eng. Mat.*, 2013, 543, 342-345.
28. X. Wu, Z. Zhang, J. Li, H. You, Y. Li and L. Chen, *Sens. Actuat. B: Chem.* 2015, 211, 507-514.
29. G. Sener, L. Uzun, R. Say and A. Denizli, *Sens. Actuat. B*, 2011, 160, 791-799.
30. B. Osman, L. Uzun, N. Besirli and A. Denizli, *Mater. Sci. Eng.*, 2013, C 33, 3609-3614.
31. Y. Taguchi, E. Takano and T. Takeuchi, *Langmuir*, 2012, 28, 7083-7088.
32. S. Öncel, L. Uzun, B. Garipcan and A. Denizli, *Ind. Eng. Chem. Res.*, 2005, 44, 7049-7056.
33. K. Hegnerová and J. Homola, *Sensor Actuat. B-Chem*., 2010, 151, 177-179.
34. L. P. Lin, L. S. Huang, C. W. Lin, C. K. Lee, J. L. Chen, S. M. Hsu and S. Lin, *Curr. Drug Targets*, 2005, 5, 61-72.
35. X. Li and S. M. Husson, *Biosens. Bioelectron*, 2006, 22, 336-348.
36. X. Wei, A. Samadi and S. M. Husson, *Sep. Sci. Technol*., 2005, 40, 109-129.
37. R. J. Umpleby, S. C. Baxter, M. Bode, J. K. Berch, R. N. Shah and K. D. Shimizu, *Anal. Chim. Acta.*, 2001, 435, 35-42.
38. G. Erturk, L. Uzun, M. A. Tumer, R. Say and A. Denizli, *Biosens. Bioelectron*, 2011, 28, 97-104.

List of Figures

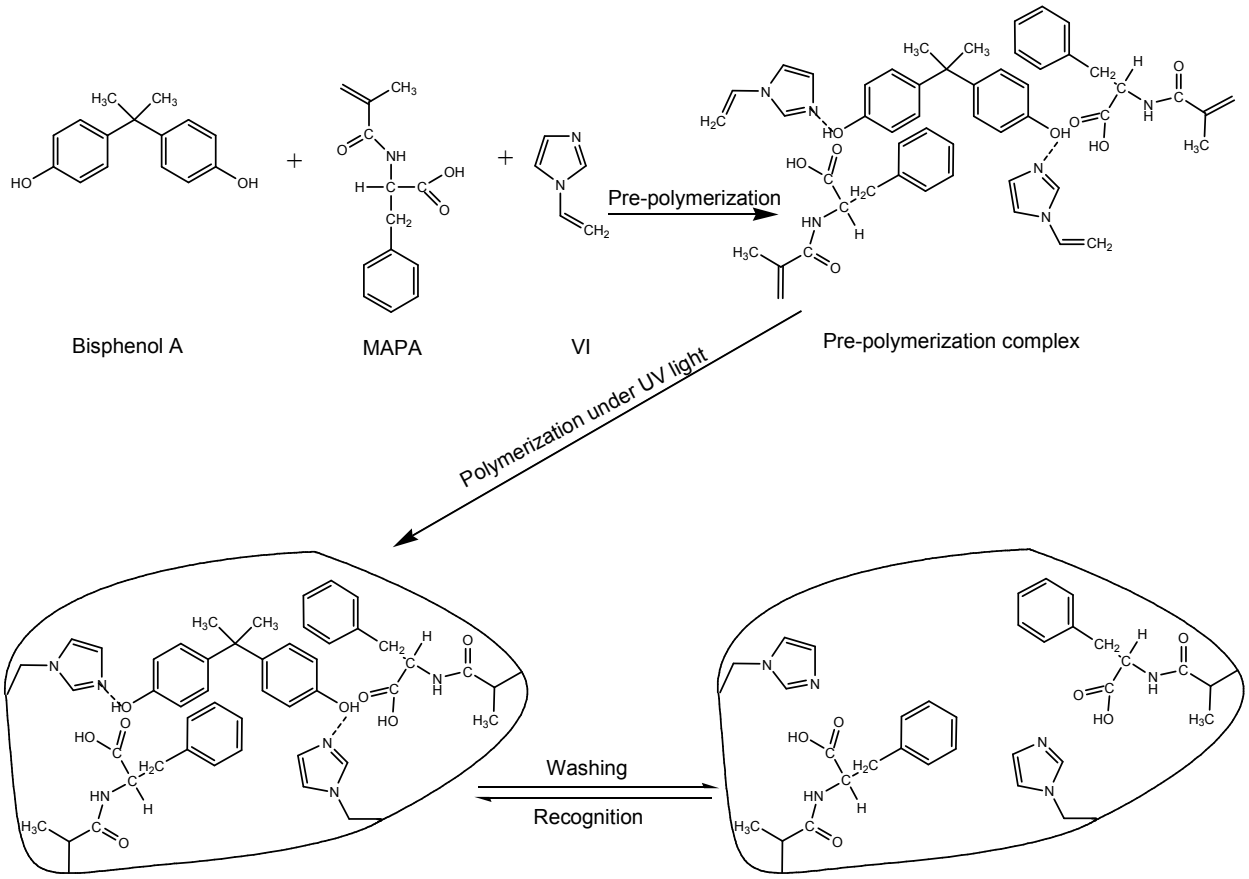

Figure 1. Schematic representation of imprinting of BPA in poly(EGDMA-MAPA-VI) nanofilm.

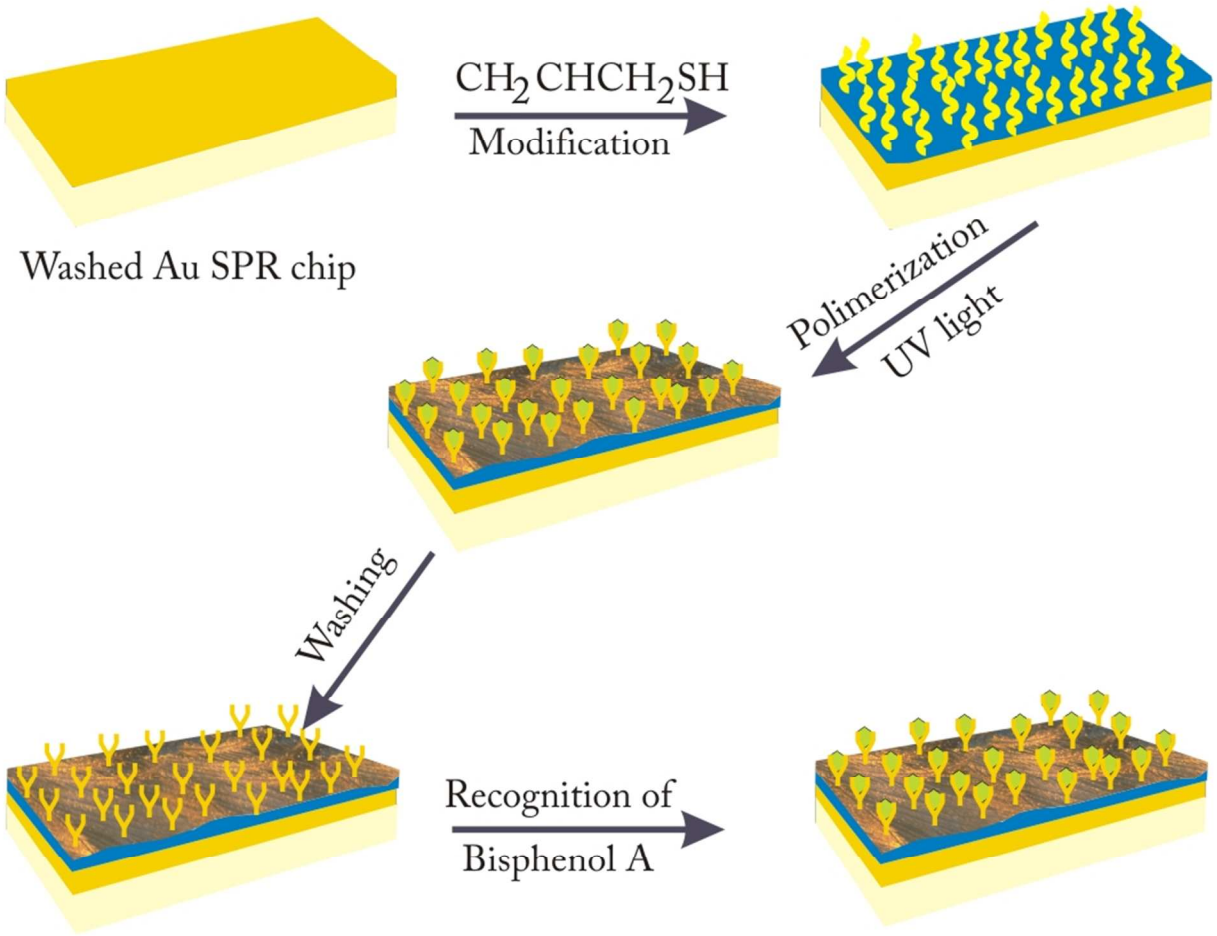

Figure 2. Steps for the preparation of BPA imprinted SPR sensor.

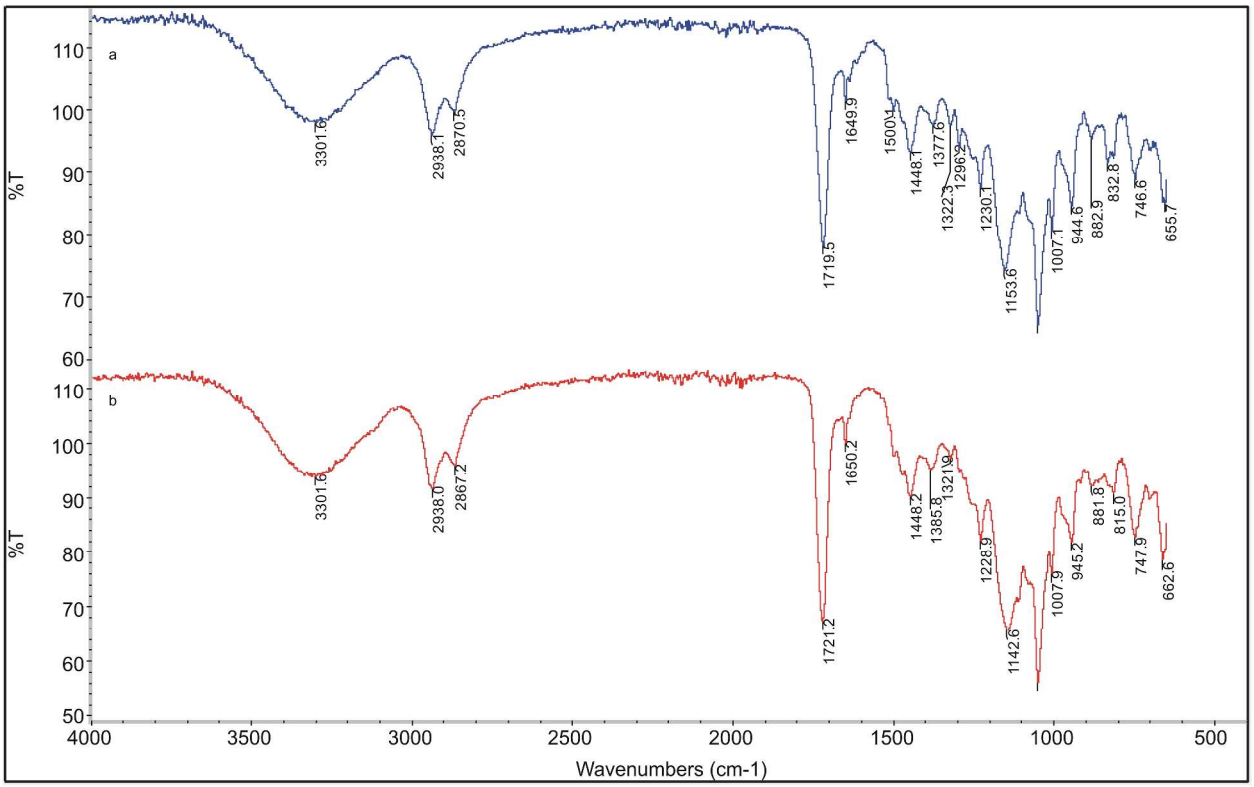

Figure 3. FTIR-ATR spectra of (a) BPA imprinted poly(EGDMA-MAPA-VI) (b) non-imprinted poly(EGDMA-MAPA-VI) nanofilm

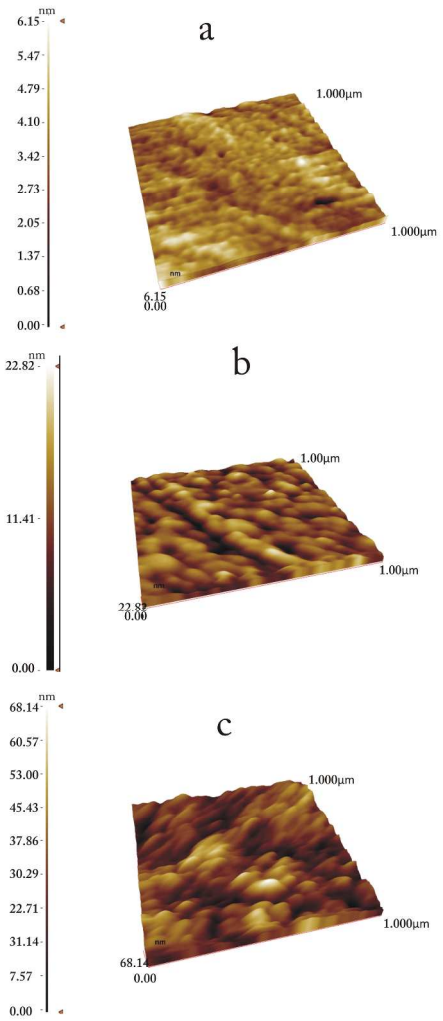

Figure 4. AFM images of (a) non-modified (b) allyl mercaptane-modified (c) BPA imprinted poly(EGDMA-MAPA-VI) nanofilm formed on SPR chip

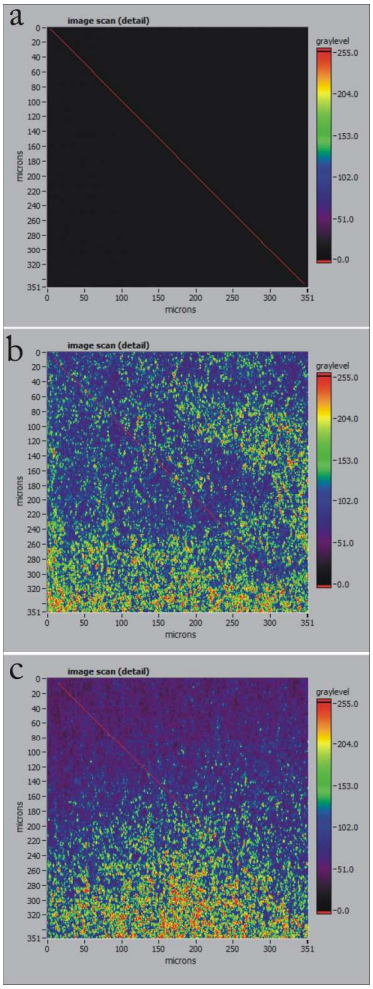

Figure 5. Image scan from ellipsometery measurements of (a) non-modified, (b) BPA imprinted poly(EGDMA-MAPA-VI) and (c) non-imprinted poly(EGDMA-MAPA-VI) modified SPR chips.

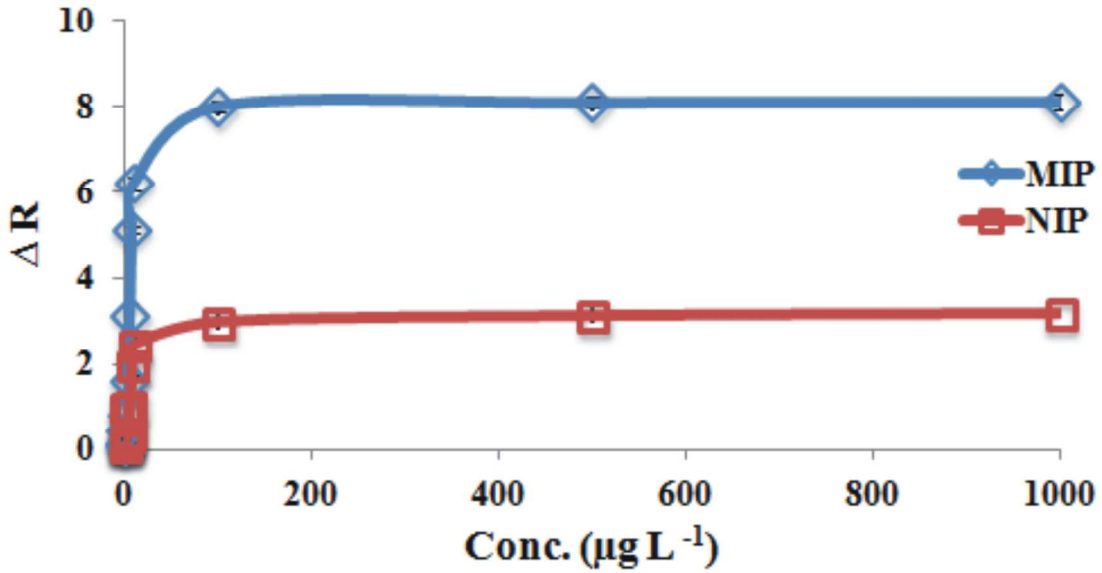

Figure 6. Response of MIP and NIP SPR sensor to different concentrations of BPA.

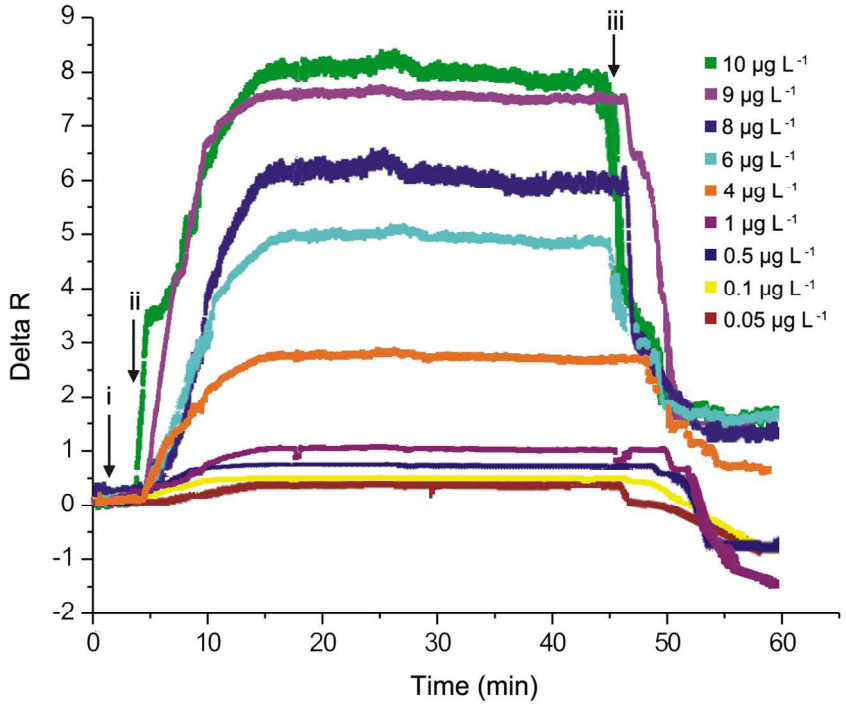

Figure 7. The sensograms for the interaction between BPA imprinted poly(EGDMA-MAPA-VI) SPR chip, (i) equilibration with water; (ii) injection of the BPA solutions; and (iii) elution with 0.2 mM NaOH.

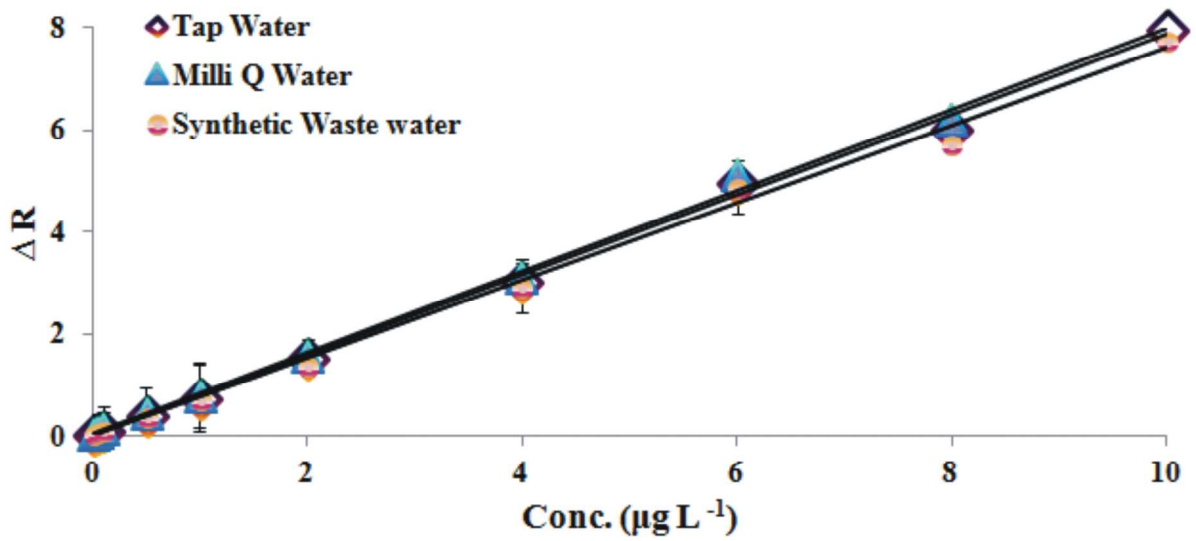

Figure 8. Standard calibration curves of BPA in milli Q water, tap water and synthetic wastewater on BPA imprinted poly(EGDMA-MAPA-VI) SPR chip.

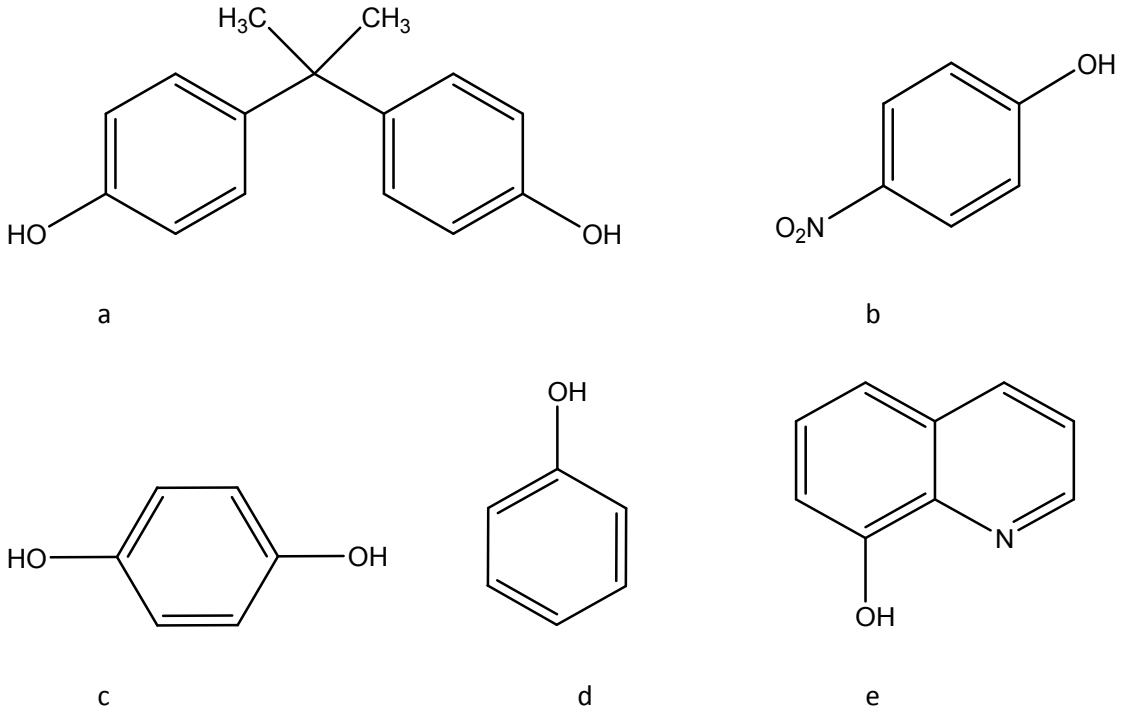

Figure 9. Chemical structures of (a) BPA (b) 4-nitrophenol (c) hydroquinone (d) phenol and (e) 8-hydroxy quinoline used in this study.

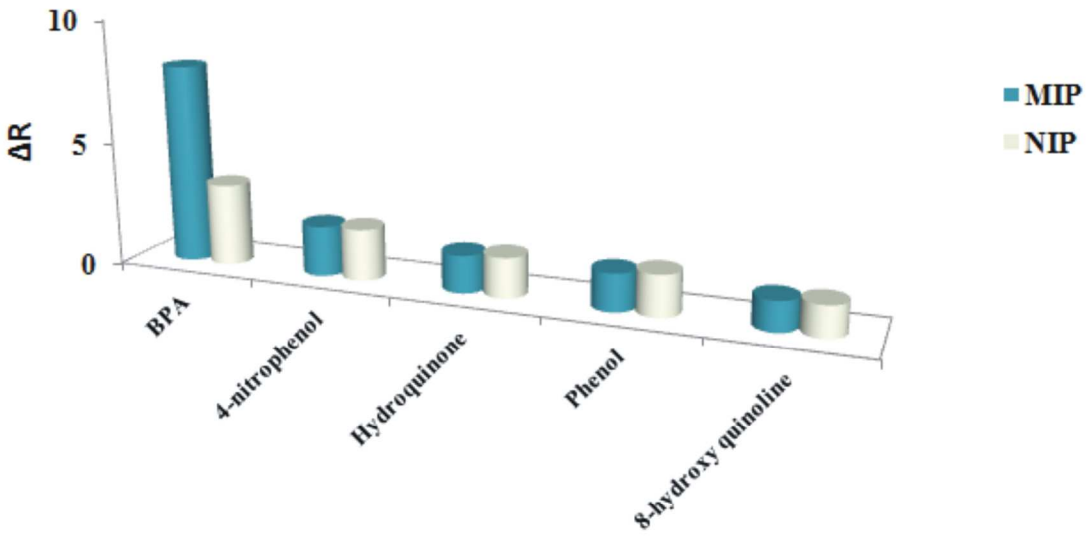

Figure 10. Selectivity of imprinted and non-imprinted poly(EGDMA-MAPA-VI) SPR sensor for BPA, 4-nitrophenol, hydriquinone, phenol and 8-hydroxy quinoline.

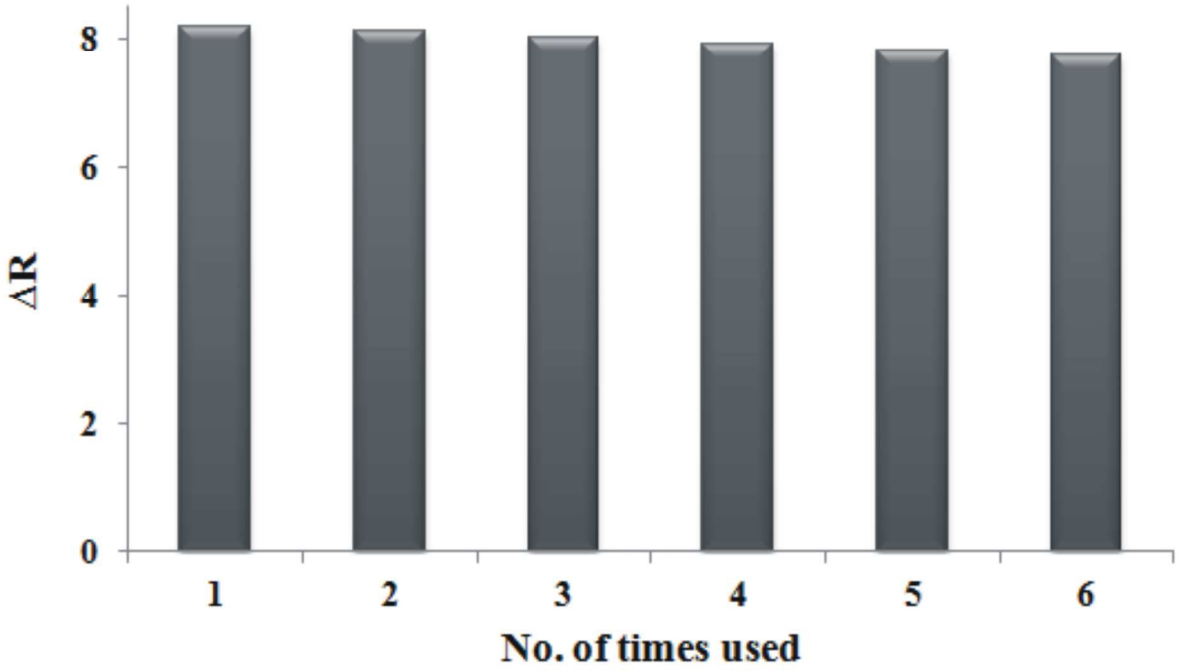

Figure 11. Reproducibility of MIP SPR sensor.

List of Tables

Table 1. Validation parameters of the BPA imprinted poly(EGDMA-MAPA-VI) SPR sensor for the determination of BPA in milli Q water, tap water and synthetic wastewater.

Validation parameters	**Milli Q water**	**Tap water**	**Synthetic wastewater**
Linear range (μg L^{-1})	0.08-10	0.2-10	0.3-10
Linearity (r^2)	0.998	0.997	0.995
Slope (a)	0.83(±0.01)	0.78(±0.013)	0.79(±0.016)
Intercept (b)	0.0065 (±0.0006)	0.015 (±0.005)	0.022 (±0.001)
LOD (μg L^{-1})	0.02	0.06	0.08
LOQ (μg L^{-1})	0.08	0.2	0.3
Intra-assay precision (% RSD)			
0.2 μg L^{-1} (n = 5)	0.15	0.43	1.03
2 μg L^{-1} (n = 5)	0.02	1.3	0.7
10 μg L^{-1} (n = 5)	0.005	0.26	0.13
Interassay precision (% RSD)			
0.2 μg L^{-1} (n = 3, 3 days)	2.2	3.76	1.4
2 μg L^{-1} (n = 3, 3 days)	1.4	2.0	1.35
10 μg L^{-1} (n = 3, 3 days)	0.65	0.5	0.16
% Recovery Lake water			
0.2 μg L^{-1}	98.7		
2 μg L^{-1}	100.6		
10 μg L^{-1}	102.7		

Table 2. Kinetic and isotherm parameters.

Association kinetic analysis		**Langmuir-Freundlich**		**Equilibrium analysis (Scatchard)**		**Langmuir**		**Freundlich**	
k_a μg L^{-1} s^{-1}	0.18	ΔR_{max} μg L^{-1}	6.74	ΔR_{max} μg L^{-1}	8.7	ΔR_{max} μg L^{-1}	8.2	ΔR_{max} μg L^{-1}	1.03
K_d s^{-1}	0.016	n	0.49	K_A μg L^{-1}	7.7	K_A μg L^{-1}	14.2	1/n	0.8
K_A μg L^{-1}	12.5	K_A μg L^{-1}	1.1	K_D L μg^{-1}	0.13	K_D L μg^{-1}	0.07	R^2	0.98
K_D L μg^{-1}	0.08	K_D L μg^{-1}	0.91	R^2	0.92	R^2	0.999		
R^2	0.999	R^2	0.999						

Table 3. The selectivity and relative selectivity coefficients of BPA imprinted poly(EGDMA-MAPA-VI) for competitor compounds.

Compounds	**ΔR MIP**	**ΔR NIP**	k_{MIP}	k_{NIP}	$k' = k_{MIP}/k_{NIP}$
Biphenol A	8.02	3.3	---	---	---
4-nitrophenol	2.2	2.05	4.0	1.6	2.5
Hydroquinone	1.5	1.6	5.35	2	2.6
Phenol	1.25	1.65	5.35	2	2.7
8-hydroxy quinoline	1.2	1.25	6.7	2.6	2.5